Mechanisms of Plastic Deformation in Ice Single Crystals

Akira HIGASHI
東　　晃
Department of Applied Physics, Faculty of Engineering, Hokkaido University
Sapporo, Japan

Abstract

A dislocation model for the mechanism of basal glide in ice single crystals is presented for interpretation of bending creep and plastic yielding experiments. The basal glide in ice single crystals is characterized by the comparatively low stress dependence of the steady strain rate, the low yield stress followed by a large yield drop and no work hardening. It was found that Johnston's theory of plastic deformation of crystals is applicable. Multiplication and movement of dislocations in the basal plane of ice crystals are discussed.

The stress-strain relation in nonbasal glide deformation is quite different from that in basal glide. The yield stress is about 20 times higher than in basal glide and the stress-strain curve shows work hardening. In the deformation process, rows of minute voids appear on the basal plane in the second stage of the stress-strain curve. The formation mechanism for these voids and their role in the deformation and fracture phenomena of ice single crystals are discussed.

I. Introduction

There have been many reports of investigations of plastic creep in poly-crystalline ice. Most of the experiments reported were conducted with the hope of applying the results to glacier movement and engineering problems in lake or sea ice. There were very few reports of experiments with single crystals of ice prior to Nakaya's (Nakaya, 1958) extensive investigation of creep in natural single crystals from the Mendenhall Glacier, Alaska. Butkovich and Landauer (1959) followed Nakaya and obtained the flow law for ice single crystals using the same material. However, understanding of the deformation mechanisms required knowledge of the stress-strain relationship. Extensive study of the mechanical properties of ice single crystals was initiated in 1960 when the Hokkaido University Glaciological Expedition led by the author, brought back about 500 kg of large ice single crystals from the Mendenhall. The first experiments covered a comparatively wide range of stress, strain rate, and temperature to investigate bending creep and the stress-strain relationship in basal glide. The results and interpretation of these experiments have been published (Higashi *et al.*, 1964, 1965), and they will be only briefly described.

In 1964, the university sent a second expedition to Alaska which brought back about 1 000 kg of large single crystals. Possession of these crystals has made it possible to continue investigation of the stress-strain relationship for nonbasal glide. Deformation behavior was found to be quite different from that in basal glide. The stress-strain curve in nonbasal glide resembles that of materials showing work hardening. Formation of minute voids was observed during the second and third stages of the curve and this

phenomenon complicates the deformation mechanism.

This paper reports a comparative study of the mechanisms of plastic deformation of ice single crystals in basal and nonbasal glide and a proposed mechanism for the void formation.

II. Experimental Procedure

a) *Material and preparation of ice specimens*

A detailed description of the natural ice single crystals used in the experiments and of the preparation of the ice specimens have been previously published (Higashi *et al.*, 1964) and will not be repeated here. However, the experiments in nonbasal glide required thinner sections than those used in basal glide experiments because the same, rather small capacity, tensile machine was used. In such thin sections, dislocations generated on the surface by mechanical polishing may be expected to penetrate the crystal deeply enough to interact with the moving dislocations in the interior, therefore, a different procedure was used. Rectangular bars ($10\times15\times60$ mm) were chemically polished at -25°C with ethyl alcohol until they reached $2.5\times15\times2$ mm. The polishing was stopped by immersing the specimen in a bath of normal hexane, also at -25°C. In this way, the mechanical strain induced by cutting the specimen from the single crystal was completely removed. Surface etching of these specimens revealed that the dislocation density was in the order of $10^3\sim10^4\,\mathrm{cm}^{-2}$ which was about one tenth of the dislocation density of the specimens used in the previous experiments.

In the non-basal glide expepiments, the crystal axes were orientated so that the *c*-axis was perpendicular to the largest face of the specimen, and so that one of the *b*-axes $\langle10\bar{1}0\rangle$, considered of primary importance in non-basal glide, were either 30, 45 or 60° to the long axis of the specimen (tensile axis).

b) *Apparatus*

The tensile testing machine designed for the stress-strain experiments is shown in Fig. 1. The strain rate was varied by using a gear system to vary the rate of ascent of the upper platform. To determine the strain rate, the motor speeds were calibrated with an inductance strain meter. The imposed stress was detected by a load cell above the upper platform and the signal was converted to an electric potential drop through a strain-gage device. The time variation of the potential drop was recorded by a recording potentiometer. Since the time scale of the chart represented the amount of tensile strain, the stress-strain relation was automatically recorded.

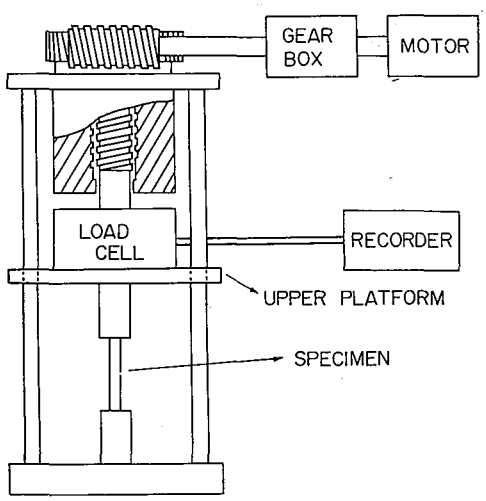

Fig. 1. Diagram of tensile testing machine

Details for the construction of the holding devices at the top and bottom of the

specimen, which are very important in tests of non-basal glide will be given in another publication. The whole tensile machine was put in a temperature box which was then placed in the cold room. The temperature in the box was maintained within ±0.1°C. The electric and electronic devices for measuring and recording the strain and stress were placed outside of the cold room.

III. Experimental Results

a) *Basal glide*

The results of experiments in bending creep and the stress-strain relation in basal glide are repeated here briefly for comparison with those at non-basal glide. Details have heen given in previous publications (Higashi *et al.*, 1964, 1965).

Creep curves were obtained with various loads at various temperatures for rectangular bars cut from ice single crystals in which the basal plane was parallel to both the bending and long axes of the bar. A typical creep curve in which the shape of the curve is characterized by an initially gentle slope followed by a steeper, constant slope is shown in Fig. 2. In this figure, the parameters which characterize the shape are ε_s, t_s and t_i. Of course, the stationary creep rate, $\dot{\varepsilon}_s$, can be obtained by the equation $\dot{\varepsilon}_s = \varepsilon_s/(t_s - t_i)$.

When the creep curves obtained at various stresses and temperatures were normalized, using $\varepsilon/\varepsilon_s$ as the ordinate and t/t_s as the abscissa, they were found to form a single curve. This indicates that ε_s and t_s are useful parameters for representing the creep curves. The temperature and stress dependence of the stationary creep rate, $\dot{\varepsilon}_s$, may be expressed by

$$\dot{\varepsilon}_s = K_1 \tau^m \exp(-Q/RT), \quad (1)$$

where T is the absolute temperature and τ the applied stress. The exponent, m, is 1.58 and the activation energy, Q is approximately 15.8 kcal/mole.

The similarity of the shapes of the creep curves to those for Ge (Penning and de Wind, 1959) and for InSb (Peissker, Haasen and Alexander, 1962) seems to indicate that Johnston's mechanism (Johnston, 1962) for plastic deformation of crystals, which states that the strain rate is determined by both the velocity of dislocation motion under stress and an increase in dislocation density with increasing strain, may be applicable. If this mechanism is valid, the eq. (1) may be derived from the following equations:

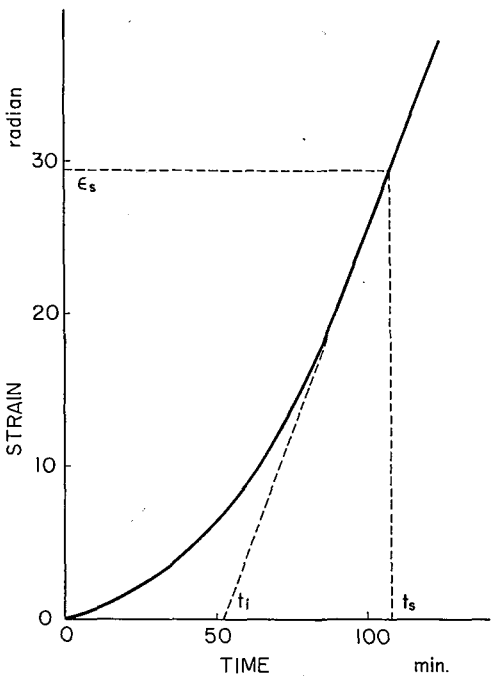

Fig. 2. Typical example of creep curves in ice single crystals in basal glide

$$\dot{\varepsilon} = 2bnv\,, \tag{2}$$

$$n = \alpha\varepsilon\,, \tag{3}$$

$$v = (\tau/D)^m, \tag{4}$$

which give the dependence of strain rate $\dot{\varepsilon}$ on dislocation-density n and velocity v as well as the dependence of dislocation density on strain ε and of dislocation velocity on stress τ. In these equations, b is the Burgers vector, α and D are constants.

If we were able to measure the stress dependence of dislocation velocity in ice single crystals directly, as has been done with LiF (Johnston and Gilman, 1959) and InSb (Chaudhuli *et al.*, 1962) etc., and if we then found the value of m to be the same as that in eq. (1), it would surely indicate that Johnston's mechanism is applicable in this instance. Unfortunately, there are not yet any reliable, direct observations of dislocation multiplication and velocity, because of the technical difficulties involved in continuous etching on an ice surface under stress, especially on the pyramidal faces on which the dislocations in motion at the basal glide emerge. However, there is an indirect way of proving that the mechanism is really taking place. The large yield drop was predictable in this case, with Johnston's theory, because of the comparatively small numerical value of m.

Typical stress-strain curves, classified by various strain rates at a constant temperature are shown in Fig. 3. Others were also obtained at different temperatures with a constant strain rate. The large yield drop is quite obvious for each curve confirming the prediction. The maximum stress on the curves, τ_{max} depends upon the strain rate and temperatures as expressed by

$$\tau_{max} = C_1 \cdot \dot{\varepsilon}^{1/m} \exp\,(E_2/RT)\,. \tag{5}$$

If this formula is converted to the equations of stress and temperature dependence of the strain rate, it becomes

$$\dot{\varepsilon} = C_2(\tau_{max})^m \exp\left(-\frac{mE_2}{RT}\right). \tag{6}$$

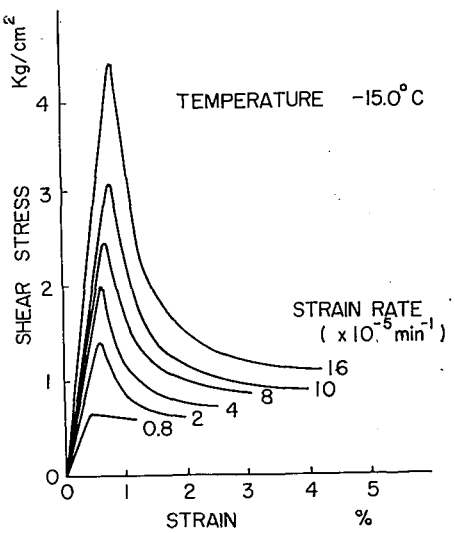

Fig. 3. Stress-strain curves for varying strain rates at constant temperature for basal glide in ice single crystal

This equation is the same type as eq. (1) and the value of m determined from the stress-strain experiments is approximately 1.53 which agrees well with the value obtained with eq. (1) and the creep experiments (1.59). The activation energy of the strain rate (mE_2 in eq. (6)), is 15.9 kcal/mole which agrees very well with that obtained from creep experiments. This agreement confirms that Johnston's mechanism of dislocation motion is taking place in basal glide in ice single crystals.

b) *Non-basal glide*

The stress-strain curves obtained for non-basal glide were not reproducible, especially in the later stages of deformation, probably because of the statistical nature of the origins

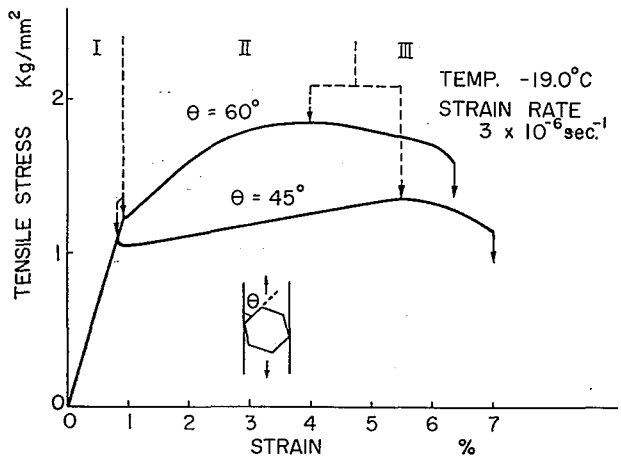

Fig. 4. Typical stress-strain curve for different orientation of the *b*-plane when the tensile axes lie in the basal plane

of the fractures. Typical curves selected from many are illustrated in Fig. 4. As may be seen the curves are divided into three parts. Initially, stage I is nearly linear with a relatively steep slope ending in slight yielding. Stage II corresponds to so called work hardening which extends to several percent of elongation. In stage III stress slowly decreases with increasing strain until fracture occurs.

This curve shape is very different from that of basal-glide and more nearly resembles that of metals and other substances showing work hardening. The yield stress is much higher than in basal-glide. A comparison of the values for yield stress in ice crystals in basal and non-basal glide with other materials is given in Table 1.

Table 1. Yield stress in various materials

Material	Upper limit, Yield stress	Exp. conditions	Investigator	Reference published
Fe	40 kg/mm²	− 78°C	Takeuchi-Ikeda	1963
Ge	5 "	+500°C	Patel-Chaudhuli	1963
LiF	0.5 "	room temp.	Johnston-Gilman	1959
Ice (non-basal)	0.9 "	−19°C, 1.8×10^{-4}min^{-1}	Mae	1967
Ice (basal)	0.04 "	−15°C, 1.6×10^{-4}min^{-1}	Higashi-Koinuma-Mae	1964

Experiments with different temperatures and strain rates elicited the curves shown in Figs. 5 and 6. The dependence of yield stress upon temperature and strain rate is expressed by

$$\tau_y = \tau_0 \cdot \dot{\varepsilon}^{1/m} \exp\left(\frac{E_3}{RT}\right). \tag{7}$$

The value for m was calculated to be $\doteqdot 7$ by the least squares method using the empirical values shown in Fig. 6. E_3 is 1.7 kcal/mole, and, therefore, the activation energy for the strain rate, mE_3, is approximately 12 kcal/mole.

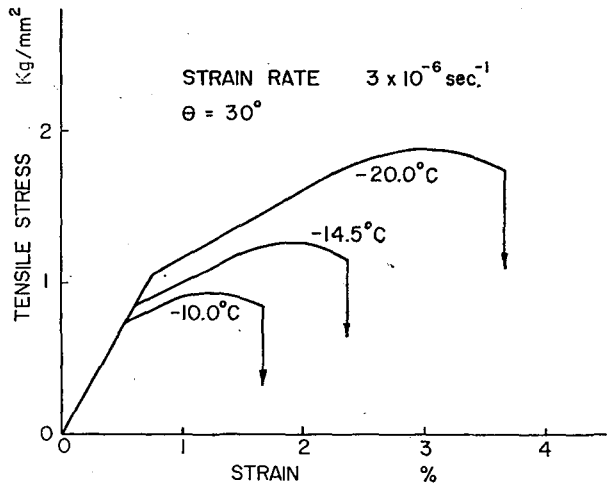

Fig. 5. Stress-strain curves for varying temperatures at constant strain rate for non-basal glide in ice single crystals

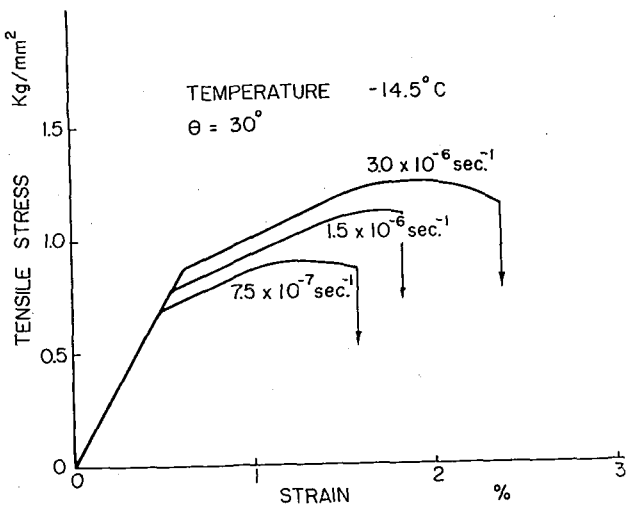

Fig. 6. Stress-strain curves for varying strain rate at constant temperature for non-basal glide in ice single crystals

The strain-hardening rate in stage II is larger when $\theta=60°$ (Curve A in Fig. 4) than when $\theta=45°$. This may prove that the b-plane $(10\bar{1}0)$ is the primary slip plane in non-basal glide. When $\theta=60°$, the symmetrical arrangement of the two slip planes $(10\bar{1}0)$ with respect to the tensile axis gives rise to greater interaction between moving dislocations than when $\theta=45°$ and there is only one $(10\bar{1}0)$ plane.

c) *Void formation in non-basal glide*

During deformation in non-basal glide, many white bands appear on the largest surface of the specimen. They are parallel to the $(10\bar{1}0)$ plane and, occasionally, perpendicular to the tensile axis. Under the microscope these lines consist of rows of thin,

minute, hexagonal, or circular, plate-shaped voids in the basal plane of the crystal (Figs. 7 and 8). Photographs taken of the prism plane (Fig. 9) reveal that the voids are in layers.

The first detectable voids appeared with a very small strain and their size and number increased and formed bands along the $\langle 11\bar{2}0 \rangle$ direction with continuing deformation in stage II. At this stage, the voids were roughly hexagonal and elongated in the direction

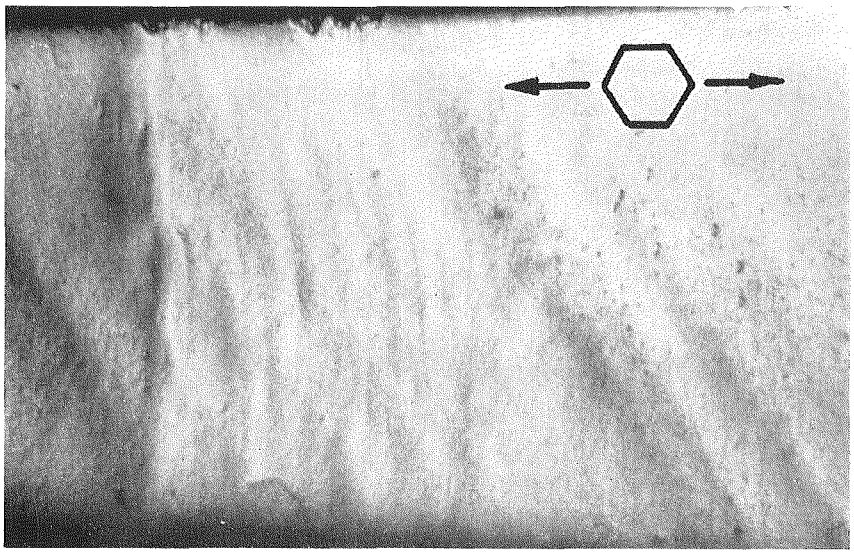

Fig. 7. Appearance of bands consisting of rows of voids along the $\langle 11\bar{2}0 \rangle$ direction, and cracks traversing in the direction normal to the tensile axis, in stage III. Tensile axis indicated by arrows. (×36)

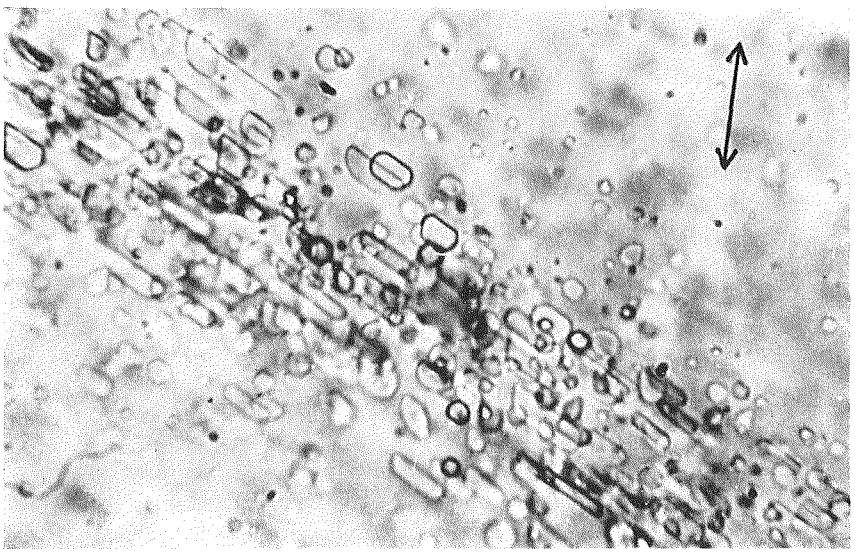

Fig. 8. Rows of thin hexagonal or circular plate-shaped voids extend along the $\langle 11\bar{2}0 \rangle$ direction in stage II. Tensile axis indicated by arrows. (×300)

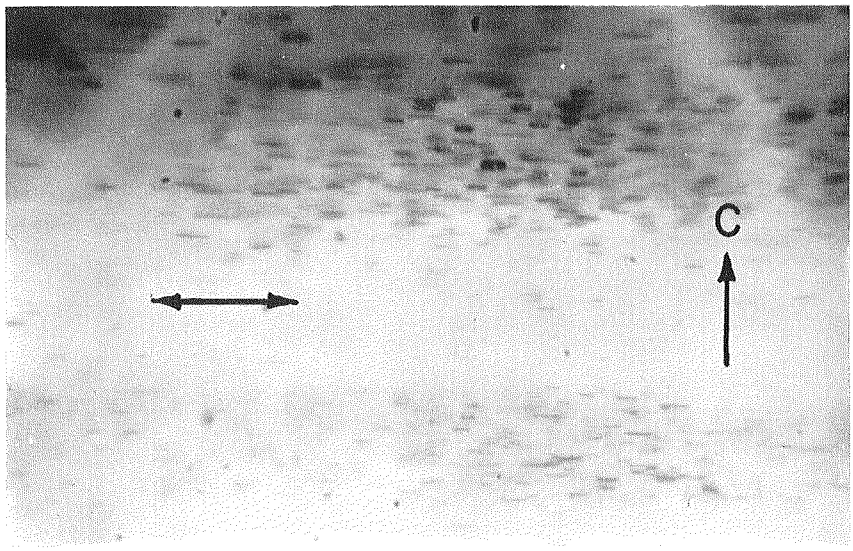

Fig. 9. Stage II, looking perpendicular to prism plane. Note rows of voids in layers. Tensile axis indicated by arrows. (×300)

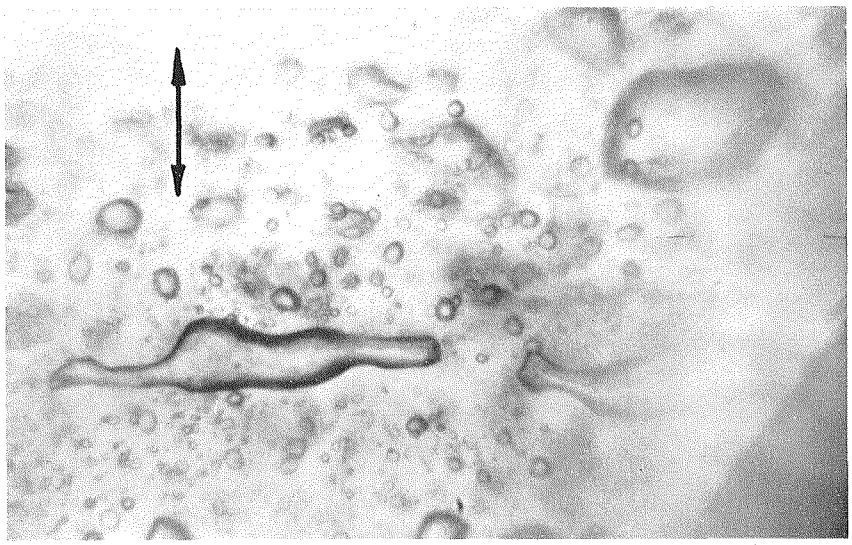

Fig. 10. Clusters of cavities formed by voids tend to extend normal to the tensile axis in stage III. Tensile axis indicated by arrows. (×300)

of the bands. In stage III the voids formed rows of cavities elongated either in the $\langle 11\bar{2}0\rangle$ direction or perpendicular to the tensile axis (Fig. 10). There is no doubt that fractures in such cases must initiate from such clusters.

When specimens were strain aged for several days at about −20°C after having reached stage III or having been fractured, it was found that the individual voids increased as much as several times their original volume, whereas the number of voids decreased. This indicates that the diffusion process is comparatively rapid.

Experiments with different strain rates revealed that visible voids appeared at higher strains with an increasing strain rate. This means that the volume of voids formed is proportional to the time of plastic deformation and also supports the diffusion process. Other experiments were carried out to study the mechanism of vacancy formation which is an elementary process in void formation. Details of these experiments will be given in a separate paper (Mae, 1967).

IV. Discussion

a) *Dislocation mechanisms in basal and non-basal glide*

The applicability of Johnston's mechanism of dislocation motion and multiplication in the case of basal glide in plastic deformation of ice single crystals was confirmed by a combination of creep and stress-strain experiments. Though the value of m (the exponent of the stress dependence of dislocation velocity) was small in this case, it still indicates that the velocity is insensitive to stress. Low yield stress and the fact that the stress-strain relation does not show a work hardening effect suggest that the dislocations on the basal plane can easily move without encountering strong obstacles.

If we assume 60° dislocations extending along $\langle 11\bar{2}0\rangle$ directions with $\langle 10\bar{1}0\rangle$ Burgers vectors as the primary dislocations on the basal plane, they are considered straight in Peierls valleys along $\langle 11\bar{2}0\rangle$, with scattered kinks between two neighbouring valleys. Since the translational motion of such dislocations is believed to occur by the longitudinal motion of kinks, the obstacles which hinder the motion of dislocations must be point defects which interact with kinks, such as vacancies, impurities, jogs, or defects at hydrogen bonds. Though it is not certain yet which defects are primary obstacles against the kink motion, it is possible to assume that the total hindrance to dislocation movement from originally existed point defects in an annealed specimen may be small because of low concentration of these defects in the crystal. In so far as the dislocations move translationally on the basal plane, they do not generate any vacancies and therefore only the equilibrium number of such defects are effective as obstacles.

Another reason for easy glide by dislocation motion on the basal plane is attributed to the comparatively long distance between pinning points on the dislocation loops, which also results from the low concentration of point defects or impurities. The force needed to move a dislocation loop is inversely proportional to the mean distance between pinning points. Strain rate also depends upon the dislocation density, which increases with the strain according to a simple assumption of eq. (3), the proportionality constant α (the rate of generation of new dislocations) also increases as the distance between pinning points increases.

In the case of non-basal glide, the mechanism of dislocation motion should be different, though the eq. (7), giving the strain rate and temperature dependence of the yield stress, has the same shape as that in the case of basal glide. The remarkable difference in the equation is that the value of exponent m in this case is larger than that for basal glide. The large value of m corresponds to the observed fact that there appears a slight yield drop, as is anticipated from Johnston's quantitative estimate based on his theory.

The difference in the stress-strain curves for basal and non-basal glide is the work

hardening effect. This fact implies that the dislocations in motion on a primary slip plane $(10\bar{1}0)$ interact with other dislocations on other primary slip planes $(1\bar{1}00)$ or $(01\bar{1}0)$. It is confirmed from the experiments on the θ dependence of the work hardening rate that this kind of cross glide occurs.

The higher value of yield stress, approximately 20 times that in the case of basal-glide (Table 1) must be due to strong obstacles against dislocation motion. In the case of the tension experiment on non-basal glide, we find climb of edge dislocations on the $\{10\bar{1}0\}$ planes. This climb generates excess vacancies in the crystal, which consequently pin the dislocations, hindering translation.

b) *Void formation by non-basal glide*

From the experimental facts that, 1) the size and number of voids increase with increasing tensile strain and 2) when a specimen including voids is strain-aged, the volume of individual voids increases whereas number of voids decreases, it can be concluded that the voids are formed by diffusion of aggregates of vacancies generated in the process of tensile deformation. Vacancies can be generated by the climb motion of edge dislocations as was stated above. This mechanism is simply illustrated in Fig. 11 and it can be easily understood that the point defects formed during dislocation climb in the tension experiment are all vacancies.

Using Friedel's calculation on the thermal equilibrium concentration of vacancies in the vicinity of climbing edge dislocations in a crystal under the tensile stress σ_t with an angle α between the tensile axis and extra half plane, the concentration C_d is given by

$$C_d = C_0 \exp\left(\frac{\sigma_t V \sin^2\alpha}{kT}\right), \qquad (8)$$

where C_0 is the thermal equiblium concentration of vacancies when climb does not occur and V the volume of one molecule. Therefore, the concentration of excess vacancies Δc at time t is given by

$$\Delta c = \rho \cdot \frac{2D_v\, t\, C_0}{n(R/r_0)} \cdot \left\{\exp\left(\frac{\sigma_t V \sin^2\alpha}{kT}\right) - 1\right\}, \quad (9)$$

where D_v is the diffusion coefficient of vacancies in the crystal, R the mean distance between dislocations, r_0 the radius of a dislocation core and ρ the dislocation density. Δc is proportional to the exponential of $\sin^2\alpha$. This dependence can be checked by taking the volumetric ratio of voids in the whole specimen as the measure of Δc. That the volume of voids at a certain value of strain (4%, $t \approx 10^4$ sec) surely differs with specimens of different α can be clearly seen in the photographs in Fig. 12. In the left photograph (a) $\theta = 60°$, or $\alpha = 30°$ while in the middle one (b) $\theta = 30°$, or $\alpha = 60°$. The density of voids is less in (a) than (b). The photograph

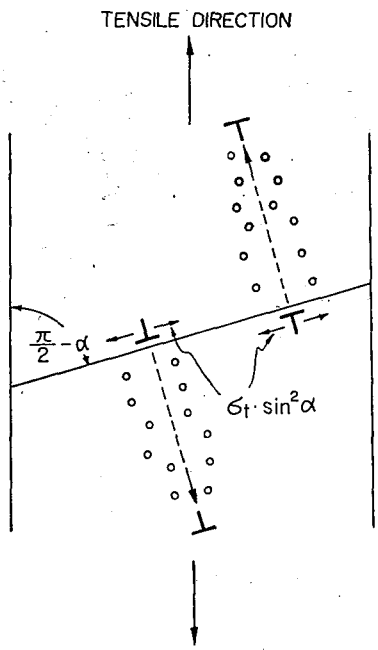

Fig. 11. Drawing of dislocation climb mechanism for formation of vacancies under tensile stress

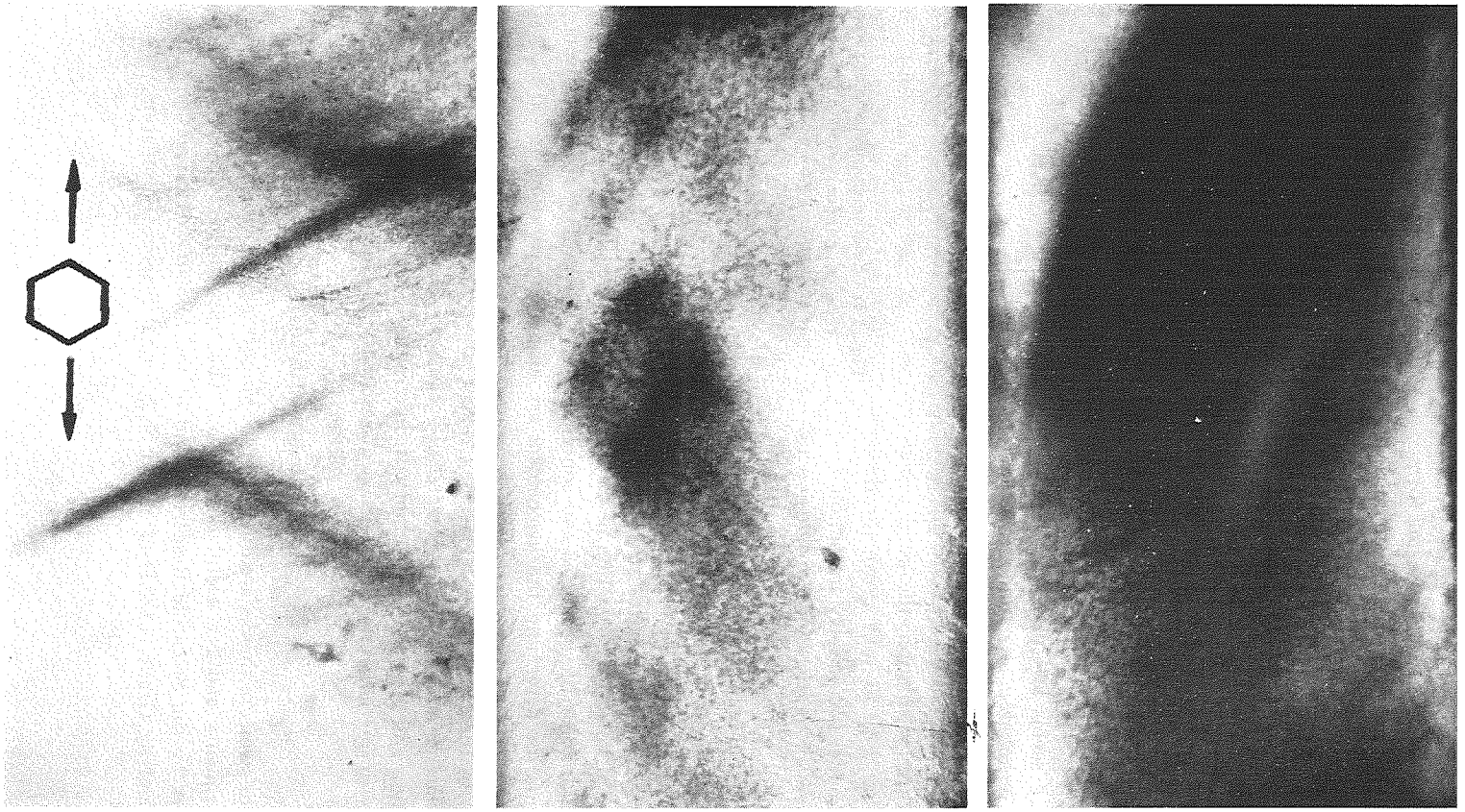

(a) (b) (c)

Fig. 12. Comparison of the density of voids formed at 4% strain with specimens of different angle α between tensile axis and extra half plane for edge dislocations on the b-plane of ice single crystal. (a $\alpha=30°$ (b) $\alpha=60°$ and (c) $\alpha=75°$. (×36)

at the right (c) is that for $\theta=15°$ or $\alpha=75°$ and appears denser shadow of voids than the former two. Comparison of calculated and empirical values of Δc with different α is illustrated in Fig. 13 and it shows a very good coincidence. Empirical values were obtained from microscopic measurements of the size and number of voids in the specimens. In the calculation, the numerical value of $D=D_v C_0$ was taken as that of tritium diffusion in ice single crystals obtained by Itagaki (1964) and the dislocation density ρ was assumed to be $10^2\ \mathrm{cm}^{-2}$. Though this value of ρ seems less than that observed, it might be reasonable to assume that some one tenth or hundredth of dislocations are edge portion which act this case. Despite this small ambiguity in the calculation, the good coincidence shown in Fig. 13 may prove the dislocation climb model for vacancy formation.

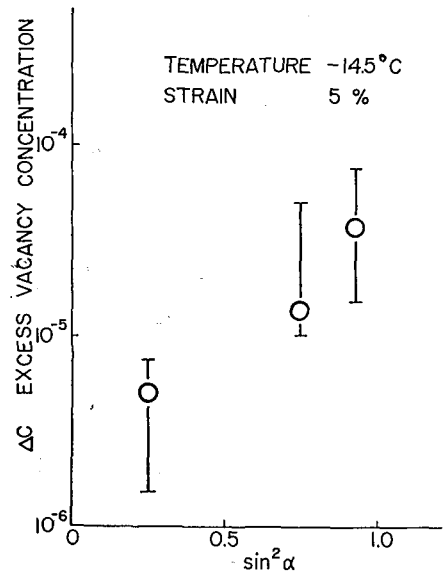

Fig. 13. Relationship between excess vacancy concentration and angle α. Calculated values indicated by circles are compared with empirical values expressed by bars indicating limits of error

The process of aggregation by diffusion to form visible voids is beyond our direct observation in the present experiments. Microscopic observation of the growth rates may be possible in tension experiments of thin specimens under a microscope. This kind of experiment as well as long term experiments of strain aging are now under way. If the dislocation climb mechanism holds for formation of vacancies in this case, the compression of specimens should not form the vacancies and consequently no voids. Compression tests, the key experiments for determing the mechanism are also in preparation.

It is interesting that the aggregates of vacancies nucleate into voids distributed along layers parallel to the basal plane. This may reflect some layer structure of the original defects which act as nuclei of the aggregates of vacancies. To make clear the mechanism of the nucleation and growth in the submicroscopic range, X-ray topographic observations are under way in our laboratory, and electrical resistivity measurements are also planned.

Acknowledgments

The author's sincere thanks are due to Dr. J. Muguruma and Mr. S. Mae for carrying out the experiments and for useful discussion. The research here described was supported in part by the Scientific Research Fund of the Ministry of Education, Japanese Government and by Grant G 18830 of the U. S. National Science Foundation.

References

1) BUTKOVICH, T. R. and LANDAUER, J. K. 1959 The flow law for ice. *SIPRE Res. Rept.*, **56**, 1–7.

2) CHAUDHULI, A. R., PATEL, J. R. and RUBIN, L. G. 1962 Velocities and densities of dislocations in Germanium and other semiconductor crystals. *J. Appl. Phys.*, **33**, 2736–2746.

3) HIGASHI, A., KOINUMA, S. and MAE, S. 1964 Plastic yielding in ice single crystals. *Japan. J. Appl. Phys.*, **3**, 610–616.

4) HIGASHI, A., KOINUMA, S. and MAE, S. 1965 Bending creep of ice single crystals. *Japan. J. Appl. Phys.*, **4**, 575–582.

5) ITAGAKI, K. 1964 Self-diffusion in single crystals of ice. *J. Phys. Soc. Japan*, **19**, 1081.

6) JOHNSTON, W. G. and GILMAN, J. J. 1959 Dislocation velocities, dislocation densities and plastic flow in Lithium Fluoride crystals. *J. Appl. Phys.*, **30**, 129–144.

7) JOHNSTON, W. G. 1962 Yield points and delay times in single crystals. *J. Appl. Phys.*, **33**, 2716–2730.

8) MAE, S. 1967 PhD Thesis, in preparation.

9) NAKAYA, U. 1958 Mechanical properties of single crystals of ice. Part 1. Geometry of deformation. *SIPRE Res. Rept.*, **28**, 1–44.

10) PATEL, J. R. and CHAUDHULI, A. R. 1963 Macroscopic plastic properties of dislocation-free Germanium and other semiconductor crystals. 1. Yield behavior. *J. Appl. Phys.*, **34**, 2788–2799.

11) PEISSKER, E., HAASEN, P. and ALEXANDER, H. 1962 Anisotropic plastic deformation of Indium Antimonide. *Phil. Mag.*, **7**, 1279–1303.

12) PENNING, P. and de WIND, G. 1959 Plastic creep of Germanium single crystals in bending. *Physica*, **25**, 765–774.

13) TAKEUCHI, T. and IKEDA, S. 1963 Yield points and transient creeps in polycrystalline iron of very low carbon content. *J. Phys. Soc. Japan*, **18**, 488–495.